Full-Wave Simulation of an Optofluidic Transmission-Mode Biosensor

Edward P. Furlani[1], R. Biswas[2] and M. Litchinitser[2]
[1]The Institute for Lasers, Photonics and Biophotonics, University at Buffalo
[2]Department of Electrical Engineering, University at Buffalo
[1]Corresponding author: 432 Natural Sciences Complex, Buffalo, NY 14260-3000, efurlani@buffalo.edu

Abstract: We present a study of an optofluidic biosensor. The sensor operates in a transmission mode wherein detection is based on a shift in the transmission spectrum caused by the contrast in refractive index between the carrier fluid and the target biomaterial. We study the behavior of the sensor using 2D full-wave electromagnetic analysis, and perform parametric studies of sensitivity as a function of key device parameters.

Keywords: optofluidic biosensor, photonic bandgap biosensor, microstructure optical fiber, ARROW waveguide biosensor.

1. Introduction

The interest in compact and portable biosensors for point-of-service clinical diagnostic applications has grown dramatically in recent years due in part to advances in microfluidics, especially lab-on-a-chip technology. A relatively new and promising approach to biosensing involves optofluidics where optic and fluidic functionality are integrated into a microsystem to leverage their combined advantages [1]. The microfluidic functionality enables compact and rapid processing of small biofluid samples, while the optical functionality enables high detection sensitivity. To date, various optofluidic biosensing platforms have been developed. Many of these utilize a detection scheme based on some form of resonant optical behavior with the input/output optical signals carried by fibers or waveguides. Examples of these include waveguide coupled photonic crystal resonators and Whispering Gallery Mode (WGM)-based sensors [2,3]. Such sensors have potential drawbacks both in terms of input/output coupling efficiency and ease of multiplexing, i.e. addressing multiple independent sensing elements in a single platform.

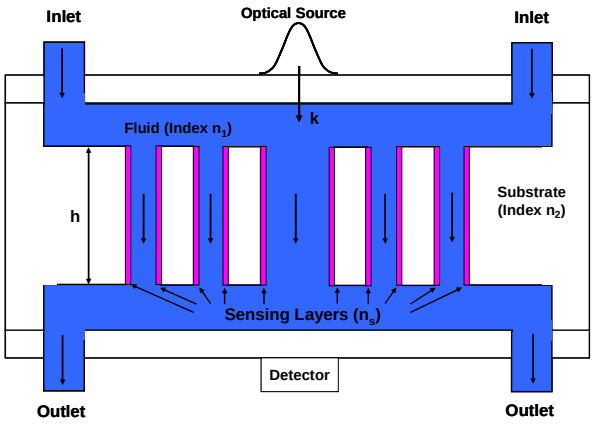

Figure 1. Microfluidic biosensor with functionalized sensing layers (crossectional view).

In this paper, we study the behavior of an optofluidic biosensor that operates in a transmission mode. The sensor consists of multiple parallel micochannels embedded in a substrate with an orientation perpendicular to its surface as shown in Fig. 1. The central microchannel is illuminated with a focused beam of light and the periodic spacing of the channels and contrast in refractive index between the fluid and the substrate act to confine and guide the incident light. The transmission spectrum of light passing through the substrate is obtained using a detector positioned beneath the central channel. The light collected in the detector depends on the dimensions, periodicity and refractive index of both the carrier fluid and the substrate material. Sensing is achieved via accumulation of a thin layer of target biomaterial on the surface of the microchannel walls, which are functionalized to bind with the material as it flows through the system. Detection is based on a shift in the transmission spectra caused by the contrast in refractive index between the carrier fluid and the thin layer of target biomaterial. We use 2D full-wave electromagnetic analysis to study the transmission sensitivity of the sensor at optical

wavelengths as a function of various device parameters. Our analysis demonstrates that a detectable shift in transmission can be achieved with relatively thin layers of target biomaterial and little contrast in refractive index between the target biomaterial and carrier fluid. As such, the sensor holds potential for compact and low-cost biosensing applications.

2. Analysis and Discussion

We use 2D full-wave time-harmonic analysis to study the field distribution and spectral response of the biosensor. For the field analysis, we use the COMSOL RF module and apply the total field formulation. We apply perfectly matched layers (PMLs) at the top and bottom of the computational domain to reduce backscatter from these boundaries (Fig. 2). Similarly, incident wave scattering boundary conditions are imposed at the boundaries transverse to the direction of propagation to reduce backscatter from these boundaries as well. We illuminate the central microchannel with a downward directed Gaussian-like beam as shown in Fig. 1. The incident field is generated by a time-harmonic surface current source positioned immediately below the upper PML with and oscillating current flowing in and out of the page as indicated in Fig. 2.

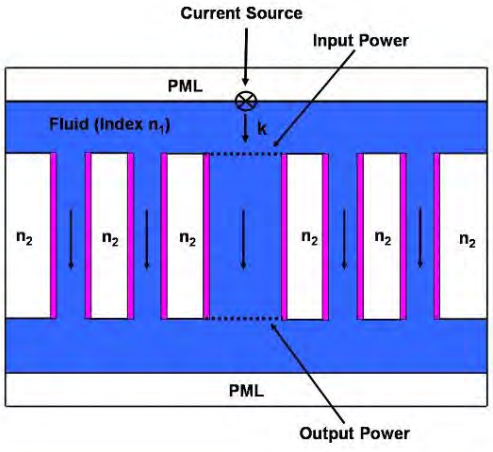

Figure 2. Computational domain.

For the initial analysis, we choose a central microchannel that has a width of 2 μm. The adjacent side channels have a width of 1 μm and are spaced 2 μm apart, center-to-center. The fluid and substrate have a refractive index of n_1 = 1.33 and n_2 =1.45, respectively. We compute the time-averaged power at the top (Input) and bottom (Output) of the central microchannel at optical wavelengths.

$$T(h,\lambda,w_s,n_s)=\frac{P_{out}(h,\lambda,w_s,n_s)}{P_{in}(h,\lambda,w_s,n_s)}. \quad (1)$$

We take the ratio of these values to determine the optical transmission $T(h,\lambda,w_s,n_s)$ through the channel., which depends on several variables including the height h of the microchannels (Fig. 1), the wavelength λ of the incident light, the width w_s of the biolayer and the index of refraction n_s of the biolayer, among others.

We first compute the transmission spectrum as a function of the channel height h. We impose a time-harmonic surface current source (flowing into the page) below the upper PML with a

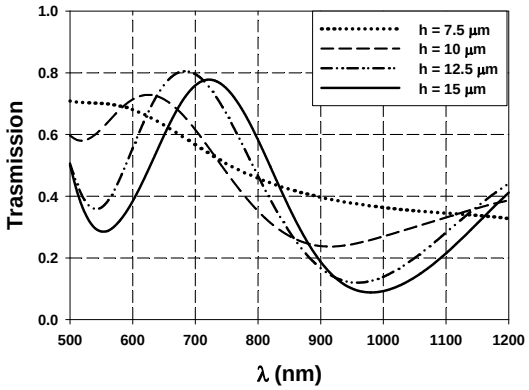

Figure 3. Transmission vs. h.

Gaussian-like profile $J = J_0 \exp\left(-\left(x/a\right)^2\right)$ where a = 1 μm. We compute the spectral response (λ = 500-1200 nm) for four different channel heights h = 7.5, 10, 12.5 and 15 μm as shown in Fig. 3. Notice that the transmission spectrum exhibits more clearly defined and pronounced maxima and minima as h increases. This is desirable for sensing as detection is based on shifts in the spectrum. This trend continues as shown in Fig. 4. However, there is a practical limit to the depth of the microchannel relative to its width, i.e. the aspect ratio is limited by microfabrication processes and material properties. For the remaining analysis we use an

aspect ratio of 15:1, and thus for 1 μm channels we limit h to 15 μm.

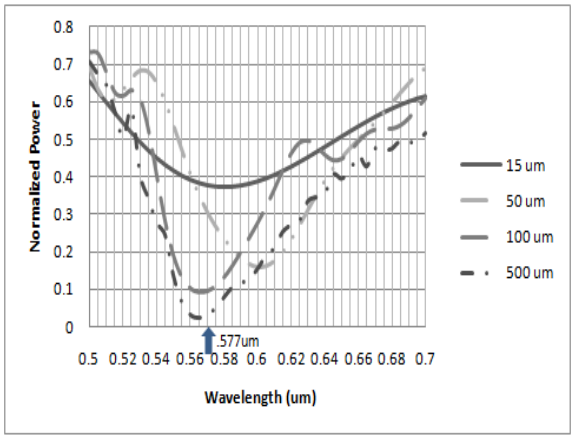

Figure 4. Transmission vs. h.

The spectral response of the sensor can be understood by recognizing that its optical configuration is similar to a 1D photonic bandgap structure [4-7]. Light launched down the low-index central microchannel (core) will be partially guided via Bragg reflections from the periodic lateral high- and low-index layers formed by the substrate and carrier fluid, respectively. As such, the spectral response can be estimated using a simple analytical expression that is derived using an antiresonant reflecting optical waveguide (ARROW) model. The transmission minima for a 1D ARROW structure are given by [4]

$$\lambda_m = \frac{2n_1 d}{m}\left[\left(\frac{n_2}{n_1}\right)^2 - 1\right]^{\frac{1}{2}} \quad (m = 1, 2, \ldots) \qquad (2)$$

where n_1 is the index of the low-index (carrier fluid) layer and d and n_2 are the width and index of the high-index (substrate) layer. It should be noted that Eq. (2) applies when $\lambda / w_c << 1$, where w_c is the width of the central microchannel. However, even though this condition is only approximately satisfied here, Eq. (2) is still useful for estimating the spectral minima. In the present analysis n_1 = 1.33, d = 1 μm and n_2 = 1.45. Thus, we estimate the first two transmission minima to occur at λ_1 = 1155 nm and λ_2 = 578 nm, respectively. The latter is indicated in Fig. 4. Note that there is a transmission minimum near λ_2 that becomes more pronounced as the channel height h increases.

Next, we perform a parametric analysis to determine the spectral response of the sensor as a function of the refractive index n_s = 1.33, 1.35,…, 1.45 of a sensing layer, which is taken

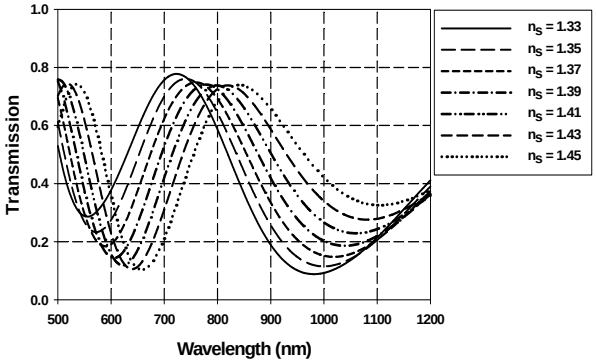

Figure 5. Transmission vs. n_s.

to be 100 nm thick. We fix h = 15 μm and compute the transmission spectra as shown in Fig. 5. Note that the transmission minima shift toward longer wavelengths as n_s increases, and that there is a decrease in transmission at λ_2.

The transmission spectra exhibit a nearly linear shift of $\Delta\lambda$ = 20 nm towards longer wavelengths for every change in refractive index $\Delta n = n_s - n_1$ = 0.02 between the sensing layer

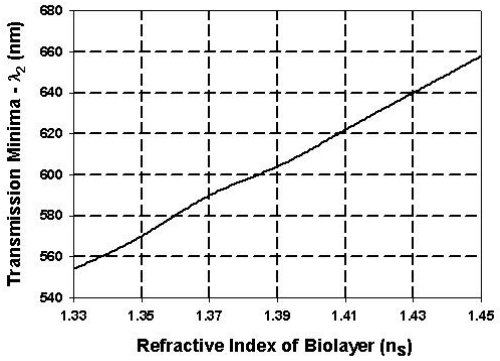

Figure 6. Transmission minima λ_2 vs. n_s.

and carrier fluid.

The index of the sensing layer can be controlled by labeling the target biomaterial with a dielectric nanoparticle of a given refractive index. If the biomaterial is labeled so that the sensing layer has the same index as the substrate ($n_s = n_2$), then the shift in the transmission spectrum can be estimated using Eq. (2), i.e

$$\Delta\lambda_m = \frac{2n_1\Delta d}{m}\left[\left(\frac{n_2}{n_1}\right)^2 - 1\right]^{\frac{1}{2}} \quad (m = 1, 2, \ldots) \qquad (3)$$

where $\Delta\lambda_m$ is the shift in the m'th minima and Δd is the effective change in width of the substrate layer, which is twice the thickness of the biolayer. For the parameters we used in our analysis above, this estimate is $\Delta\lambda_2$ = 115.6 nm.

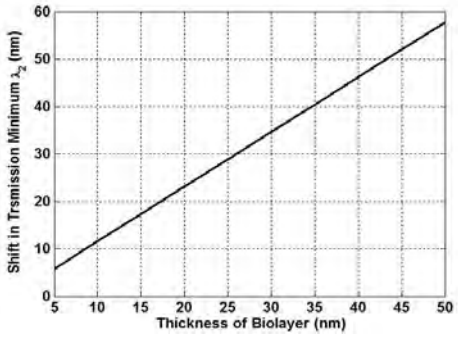

Figure 7. Shift in λ_2 vs. biolayer thickness.

Our computed shift was $\Delta\lambda = 104$ nm. We use Eq. (3) to estimate the shift in λ_2 as a function the thickness of the biolayer with $n_s = n_2$. This plot is linear with a slope $\sqrt{\left(n_2^2 - n_1^2\right)}$ as shown in Fig. 7.

This preliminary analysis indicates that detectable shifts in transmission can be achieved with thin (nm) layers of target biomaterial. Additional analysis is needed to determine optimum device parameters that are compatible with optical illumination and detection methods, and that can realized using conventional materials and fabrication processes. Device optimization can be accomplished using the COMSOL RF module, and parametric designs can be completed within a few minutes on a modern workstation.

4. Conclusions

The field of optofluidics is its infancy and growing rapidly. Optofluidic microsystems hold substantial potential for biosensing applications as the optical functionality enables high detection sensitivity of small biosamples. In this paper we have introduced an optofluidic transmission mode biosensor and we have studied its performance using 2D full-wave electromagnetic analysis. Our results indicate that a detectable shift in transmission can be achieved with thin layers of biomaterial and relatively low contrast between the biomaterial and carrier fluid. The analysis takes only a few minutes to perform on a modern workstation, and can be used to optimize the sensitivity of the biosensor for various applications.

References

[1] C. Monat, P. Domachuk and B. J. Eggleton Integrated optofluidics: A new river of light Nature Photonics **1** 2, 106-114 (2007).

[2] F. Vollmer, D. Braun, A. Libchaber, M. Khoshsima, I. Teraoka, and S. Arnold, Protein detection by optical shift of a resonant microcavity, App. Phys. Lett. **80** 4057-4059 (2002).

[3] M. R. Lee, P. Fauchet, Two-dimensional silicon photonic crystal based biosensing platform for protein detection, Opt. Express **15**, 4530-4535 (2007)

[4] N. M. Litchinitser, A. K. Abeeluck, C. Headley, and B. J. Eggleton, Antiresonant reflecting photonic crystal optical waveguides, Opt. Lett. **27**, 1592 (2002).

[5] J A. M. Zheltikov, Ray-optic analysis of the biosensing ability of ring-cladding hollow waveguides, Appl. Opt. **47**, 3 474-479 (2008).

[6] N. Litchinitser, S. Dunn, P. Steinvurzel, B. Eggleton, T. White, R. McPhedran, and C. de Sterke, Application of an ARROW model for designing tunable photonic devices, Opt. Express **12**, 1540 (2004).

[7] N. M. Litchinitser and E. Poliakov, Antiresonant guiding microstructured optical fibers for sensing applications, Appl. Phys. B **81**, 347-351 (2005).